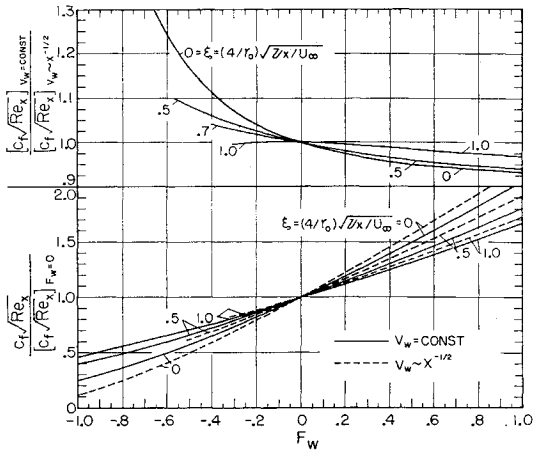

Fig. 2 Effect of surface mass transfer on skin friction.

transfer parameter F_w, and the curves are parameterized by ξ. The case $\xi = 0$ corresponds to the flat plate. By inspecting the figure, one sees that the general effect of blowing ($F_w < 0$) is to decrease the skin friction, whereas suction ($F_w > 0$) increases the skin friction. Further study shows that, for a given value of the F_w parameter, the effect of surface mass transfer is diminished as ξ increases. Thus, the flat plate is most affected by surface mass transfer and cylinders ($r_0 < \infty$) are affected to a lesser extent.

The essential point of this finding is that surface mass transfer and transverse curvature oppose one another. In the case of blowing, the boundary layer is thickened and the skin friction is reduced; however, the thickening of the boundary layer accentuates the transverse curvature effect, which in turn tends to increase the skin friction. The net effect is a reduction in skin friction, but to an extent that is less than that for the flat plate.

Next, attention may be directed to a comparison of results for the two distributions of surface mass transfer as shown in the upper portion of Fig. 2. The ordinate is the ratio of $c_f\, Re_x^{1/2}$ for uniform mass transfer to $c_f\, Re_x^{1/2}$ for the $v_w \sim x^{-1/2}$ mass-transfer distribution. In general, it appears that the $x^{-1/2}$ distribution is somewhat more effective in increasing skin friction by suction and decreasing skin friction by blowing than is the uniform distribution. However, aside from the flat plate with blowing, the results are remarkably insensitive to the detailed distribution of the surface mass transfer.

Numerical values of the displacement thickness cannot be reported here because of space limitations, but these are available in Ref. 4. As a final remark, it is of interest to note that the present investigation extends the range of results for uniform blowing for the flat plate. Previous information, obtained by a finite-difference solution[5] was restricted to $F_w = -0.141$ and -0.283.

References

[1] Lew, H. G., "The asymptotic behavior of the boundary layer to transverse curvature," J. Aeronaut. Sci. **23**, 276–277, 895–897 (1956).

[2] Steiger, M. H. and Bloom, M. H., "On thick boundary layers over slender bodies with some effects of heat transfer, mass transfer, and pressure gradient," Intern. J. Heat Mass Transfer **5**, 513–520 (1962).

[3] Seban, R. A. and Bond, R., "Skin friction and heat transfer characteristics of a laminar boundary layer on a cylinder in axial incompressible flow," J. Aeronaut. Sci. **18**, 671–675 (1951).

[4] Wanous, D. J., "Heat transfer and skin friction for longitudinal flow over a cylinder with surface mass transfer," M.S. Thesis, Dept. of Mechanical Engineering, Univ. of Minnesota (1963).

[5] Lew, H. G. and Fanucci, J. B., "On the compressible boundary layer over a flat plate with suction and injection, J. Aeronaut. Sci. **22**, 589–597 (1955).

A Practical Note on the Use of Lambert's Equation

GEZA S. GEDEON*
Northrop Space Laboratories, Hawthorne, Calif.

Nomenclature

μ = $\cong GM$ product of universal gravitational constant and mass of principal attracting body
e = eccentricity
a = semimajor axis
r = separation from the dynamical center
c = chord
s = $(r_0 + r + c)/2$ = semiperimeter
z = $s/2a$ = argument of the Lambertian series
w = $(1 - c/s)^{1/2}$ = shape factor
n_s = $(\mu/s^3)^{1/2}$ = mean motion based on semiperimeter
A_n = $\dfrac{1\cdot 3\cdot 5 \ldots (2n-1)}{2\cdot 4\cdot 6 \ldots (2n)}$; $A_0 = 1$
N = $n_s t$ = mean anomaly based on semiperimeter
α, β = Lambert's angles for elliptic orbits
γ, δ = Lambert's angles for hyperbolic orbits
k = ± 1
m = 1, 2 . . . integer

WHEN the time of flight is given between two terminals, the equations of Lambert are used to determine the orbit. These equations, however, have several drawbacks, and the following will show how to overcome these difficulties without compromising the simplicity of the original expressions.

Lambert's equations are the following:

Hyperbolic Orbits

$$t = (|a|^3/\mu)^{1/2}[(\sinh\gamma - \gamma) - (\sinh\delta - \delta)] \tag{1}$$

$$\sinh(\gamma/2) = (s/2|a|)^{1/2} \qquad \sinh(\delta/2) = [(s-c)/2|a|]^{1/2} \tag{2}$$

Parabolic Orbits

$$t = \tfrac{1}{3}(2/\mu)^{1/2}[s^{3/2} \mp (s-c)^{3/2}] \tag{3}$$

Elliptic Orbits

$$t = (a^3/\mu)^{1/2}[(1-k)m\pi + k(\alpha - \sin\alpha) \mp (\beta - \sin\beta)] \tag{4}$$

$$\sin\frac{\alpha}{2} = \left(\frac{s}{2a}\right)^{1/2} \qquad \sin\frac{\beta}{2} = \left(\frac{s-c}{2a}\right)^{1/2} \tag{5}$$

where $k = \pm 1$ and $m = 1, 2 \ldots$ integer number of loops (see, e.g., Ref. 1).

To solve these equations for a on an automatic digital computer, the fast and efficient Newton-Raphson method can be applied if the derivatives are available. To obtain these derivatives, the auxiliary equations (2) and (5) will be eliminated by the introduction of the variable

$$z = s/2a \tag{6}$$

and the constants

$$w = \pm(1 - c/s)^{1/2} \qquad n_s = (\mu^3/s)^{1/2} \tag{7}$$

With these substitutions, Eqs. (1) and (4) and their derivatives can be written in the combined form

$$N = n_s t = \frac{1}{z|z|^{1/2}\,2^{1/2}}\left\{\frac{1-k}{2}m\pi + k[f(|z|^{1/2}) - |z|^{1/2}(1-z)^{1/2}] - [f(w|z|^{1/2}) - w|z|^{1/2}(1-w^2z)^{1/2}]\right\} \tag{8a}$$

Received April 6, 1964; revision received August 21, 1964.

* Chief, Flight Mechanics Group. Associate Fellow Member AIAA.

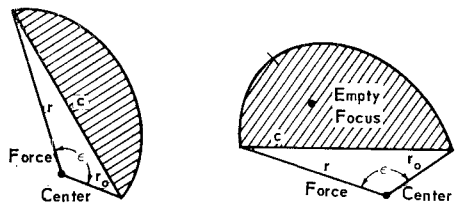

Fig. 1 Geometry of elliptic trajectories.

and

$$\frac{dN}{dz} = \frac{1}{|z|2^{1/2}}\left\{\frac{k}{(1-z)^{1/2}} - \frac{w^3}{(1-w^2z)^{1/2}} - \frac{3N}{2^{1/2}}\right\} \quad (8b)$$

In these equations, for hyperbolic orbits, f = arcsinh, $k = +1$, and for elliptic orbits, f = arcsin, $k = \pm 1$.

These equations are free from ambiguity if it is agreed that $k = +1$ when the empty focus falls outside the area enclosed by the chord and the trajectory and $k = -1$ if it falls inside of it. Also w is positive if the central angle is less than π and negative if greater than π (see Fig. 1). Finally, Eq. (3) with the new notation becomes

$$N = (2^{1/2}/3)(1 - w^3) \quad (9)$$

For $z \backsimeq 0$, Eqs. (8) exhibit undeterminancy problems that can be eliminated by broadening the region of validity of Eq. (9).

From Eq. (8a) with $k = +1$, and permitting $z^{1/2}$ to take on imaginary values, one gets

$$\frac{d(z^{3/2}N)}{dz} = \frac{1}{2^{1/2}}\left\{\frac{z^{1/2}}{(1-z)^{1/2}} - \frac{w^3\, z^{1/2}}{(1-w^2z)^{1/2}}\right\} \quad (10)$$

Expanding Eq. (10) around $z = 0$ by

$$(1-z)^{1/2} = \sum_{n=0}^{\infty} A_n z^n$$

$$\text{where } A_0 = 1 \qquad A_n = \frac{1\cdot 3\cdot 5 \ldots (2n-1)}{2\cdot 4\cdot 6 \ldots (2n)} \quad (11)$$

it becomes

$$\frac{d(z^{3/2}N)}{dz} = \frac{z^{1/2}}{2^{1/2}}\left\{\sum_{n=0}^{\infty} A_n z^n - w^3 \sum_{n=0}^{\infty} A_n w^{2n} z^n\right\} \quad (12)$$

which can be integrated to yield

$$z^{3/2}N = \frac{1}{2^{1/2}}\left\{\sum_{n=0}^{\infty} \frac{A_n}{n+3/2}(1 - w^{2n+3})z^{n+3/2}\right\} + C \quad (13)$$

The constant of integration for $z = 0$ is obtained as $C = 0$. Then dividing by $z^{3/2}$ the result is (see also Ref. 2)

$$N = 2^{1/2} \sum_{n=0}^{\infty} \frac{A_n}{2n+3}(1 - w^{2n+3})z^n \quad (14a)$$

The derivative of this equation is

$$\frac{dN}{dz} = 2^{1/2} \sum_{n=1}^{\infty} \frac{nA_n}{2n+3}(1 - w^{2n+3})z^{n-1} \quad (14b)$$

Now Eq. (14) is valid between $z = -1$ and $+1$, where the power series converges. Note, however, that near the limits the convergence is very slow.

Finally, the question of which equation to use and with what value of z to begin the iteration emerges. To answer this question, three numbers must be calculated which are related to $z = -1, 0, +1$:

$$N_{-1} = 1 - (1/2^{1/2})\{(\sinh^{-1}1 - \sinh^{-1}w) + w(1+w^2)^{1/2}\} \quad (15)$$

$$N_0 = (2^{1/2}/3)(1 - w^3) \quad (16)$$

$$N_{+1} = (1/2^{1/2})\{\pi/2 - \sin^{-1}w + w(1-w^2)^{1/2}\} \quad (17)$$

Defining $\Delta = (N_0 - N_{-1})$, the following trouble-free regimes and initial z values can be recommended:

1) $N < \left[N_{-1} + \left(\frac{\Delta}{4}\right)\right]$, use the hyperbolic form of Eqs. (8) with $z_i = -1$ and $k = +1$.

2) $\left[N_{-1} + \left(\frac{\Delta}{4}\right)\right] \leq N < \left(N_0 + \Delta\right)$, use the parabolic form of Eqs. (14) with $z_i = 0$

3) $(N_0 + \Delta) \leq N < N_{+1}$, use the elliptic form of Eqs. (8), with $z_i = 0.75\ k = +1$

4) $N_{+1} \leq N$, use the elliptic form of Eqs. (8), with $z_i = 0.75$ and $k = -1$ and m according to the problem.

References

[1] Battin, R. H., *Astronautical Guidance* (McGraw-Hill Book Co., Inc., New York, 1964).

[2] Gedeon, G. S., "Lambertian mechanics," *Proceedings of the XII International Astronautical Congress* (Springer-Verlag, Wien, and Academic Press Inc., New York, 1963).

Determination of Mass Eroded from Pulsed Plasma Accelerator Electrodes

T. L. Rosebrock,* D. L. Clingman,† and D. G. Gubbins‡
General Motors Corporation, Indianapolis, Ind.

A NOVEL method has been devised for the capture of plasma discharge products for subsequent determination of the eroded electrode mass. The technique also permits simultaneous measurement of the plasma linear momentum for the accelerator considered.

The apparatus consisted of a ballistic pendulum with a cylindrical bob, the axis of which was colinear with the accelerator axis. The pendulum bob was lined with chemically pure filter paper and completely surrounded the discharge zone, including the electrodes. The accelerator consisted of two parallel cylindrical 0.006-m-diam electrodes, 0.2 m in length, spaced on 0.025 m centers. The electrodes were connected through a coaxial spark gap switch to a 6.4-μf capacitor charged to 15 kv. Propellant materials were 1-mil-diam silver wires 0.019 m in length. All experiments were carried out at pressures of 5×10^{-5} torr or less.

The propellant mass accelerated in a typical discharge was on the order of 10^{-7} kg. Since it was assumed that the eroded mass was only a small fraction of the propellant mass (this assumption was subsequently confirmed by the experiment), samples were prepared by accumulating the discharge products of ten successive shots, and an average value of the eroded mass determined therefrom.

A trend of increasing momentum with accumulated firings had been observed[1] when the electrodes were not cleaned and polished between firings. After about 30 shots, the momentum stabilized at a value approximately 10% above the initial value. In order to determine if a correlation existed between erosion and momentum change, deposits were collected for

Presented as Preprint 64-708 at the AIAA Fourth Electric Propulsion Conference, Philadelphia, Pa., August 31–September 2, 1964; revision received August 19, 1964.

* Principal Scientist, Magnetoplasmadynamic Research, Allison Division. Member AIAA.

† Senior Research Scientist, Magnetoplasmadynamic Research, Allison Division. Member AIAA.

‡ Senior Research Scientist, Magnetoplasmadynamic Research, Allison Division.